JOURNAL OF APPLIED ELECTROCHEMISTRY **15** (1985) 217–223

Electrodeposition of catalytically active nickel–thallium alloy powders from sulphate baths

A. M. ABD EL-HALIM,* R. M. KHALIL

Department of Chemistry, Faculty of Science, King Abulaziz University, Jeddah, Saudi Arabia

Received 25 April 1984; revised 7 June 1984

The electrodeposition of nickel–thallium alloy powder was investigated from acidic sulphate baths containing 0.0125 $NiSO_4 \cdot 6H_2O$, 0.005–0.020 Tl Cl, 0.05–0.23 $(NH_4)_2SO_4$, 0.1 H_3BO_3 and 0.07 mol l^{-1} $Na_2SO_4 \cdot 10H_2O$. The polarization curves, the percentage composition and the current efficiency of the electrodeposited alloy powders were determined as a function of the bath composition. In addition, some properties of the deposits were examined such as the surface morphology, the structure as revealed by X-ray diffraction analysis and the catalytic activity towards the decomposition of 0.4% H_2O_2 solution. The results indicate that the characteristics of the alloy deposition and the properties of the alloy powder are affected to different extents by the bath composition.

1. Introduction

The standard electrode potentials of nickel (− 0.250 V) and thallium (− 0.336 V) are only about 0.086 V apart and consequently their codeposition from acidic baths is feasible. Nevertheless, only a few studies on the electrodeposition of nickel–thallium alloys have been made [1–3]. In general, the electrodeposition of thallium or its alloys is of limited commercial importance [4]. This is because the deposits from acidic baths are noncoherent and of mossy or dendritic nature [4, 5]. Therefore thallium is exploited as a grain refiner for example, in the electrodeposition of gold [6]. In addition, electrodeposited nickel–thallium alloys containing ^{204}Tl were recommended as a source of β-radiation [7].

In a recent paper [8] we reported an optimum bath composition, denoted as Bath Ni-1 in Table 1, suitable for recovery of nickel powders from industrial effluents. The current efficiency of this bath was relatively low and the nickel powders were characterized by a moderate catalytic activity. Later, we carried out a detailed study [9] on the electrodeposition of thallium powders from a bath of similar composition, denoted as Bath Tl-1 in Table 1. This study led to the conclusion that finer-grained thallium powders could be electrodeposited under the same conditions as for nickel. Accordingly, the present investigation was undertaken to investigate further the electrodeposition of nickel–thallium alloy powders in an attempt to find the optimum bath composition for this process. Thallium plays the role of a grain refiner and is expected to improve the efficiency of the bath and the catalytic activity of the alloy deposit.

2. Experimental details

The baths used for electrodeposition of the parent metals and the alloy were prepared from AnalaR grade chemicals (BDH) and distilled water. The compositions, pHs and specific conductance of these baths are given in Table 1. The experimental arrangement for electrodeposition consisted of a Perspex cell with a copper cathode positioned midway between two plane parallel nickel anodes; all electrodes were of the same geometrical area.

The polarization curves, relative to a saturated calomel electrode (SCE), were determined with a Wenking potentioscan model POS 73 and recorded automatically by means of a Philips *x–y* recorder model PM 8132. The composition of each electrodeposited alloy was determined by means of an atomic absorption spectrophotometer model 5000, Perkin-Elmer. The cathodic current efficiency

---

*Permanent address: Department of Chemistry, Faculty of Science, Ain Shams University, Abbassia, Cairo, Egypt.

Table 1. Composition, pH and specific conductance (C) of the metal and alloy deposition baths

Bath	*Concentrations* ($mol\,l^{-1}$)					*pH*	C ($ohm^{-1}\,cm^{-1}$)
	$NiSO_4 \cdot 6H_2O$	$TlCl$	$(NH_4)_2SO_4$	H_3BO_3	$Na_2SO_4 \cdot 10H_2O$		
Ni-1	0.0125	–	0.23	0.10	0.07	4.80	0.041
Tl-1	–	0.010	0.23	0.10	0.07	4.80	0.036
(Ni–Tl)1	0.0125	0.010	0.23	0.10	0.07	4.80	0.046
(Ni–Tl)2	0.0125	0.010	0.15	0.10	0.07	4.85	0.032
(Ni–Tl)3	0.0125	0.010	0.10	0.10	0.07	4.90	0.029
(Ni–Tl)4	0.0125	0.010	0.05	0.10	0.07	4.90	0.020
(Ni–Tl)5*	0.0125	0.005	0.10	0.10	0.07	3.00	0.029
(Ni–Tl)3a*	0.0125	0.010	0.10	0.10	0.07	3.00	0.037
(Ni–Tl)6*	0.0125	0.020	0.10	0.10	0.07	3.00	0.205

*The pH of these baths was adjusted by additions of concentrated H_2SO_4 (98%).

(*f*%) was determined by using a standard copper coulometer. The morphology of the as-deposited powders was examined with a scanning electron microscope (JEOL model JSM 35). X-ray diffraction studies were carried out by a Philips X-ray diffractometer PW 1390, with a nickel filter and copper radiation. The percentage decomposition (*D*%) of 0.4% H_2O_2 solution (at 40° C) on the surface of the electrodeposited powders was considered as a measure of their catalytic activity. Therefore, a definite volume (50 ml) of the H_2O_2 solution was passed (single-pass) over a fixed bed (0.15 g) of the test powder with a constant flow-through rate ($150\,ml\,h^{-1}$) by the aid of a peristaltic pump (LKB Bromma model 2132). The *D*% was calculated by measuring the exact concentrations of H_2O_2 spectrophotometrically before and after its passage over the powders. Unless otherwise stated, all types of measurements were carried out at room temperature.

3. Results and discussion

3.1. *Polarization curves*

Fig. 1 shows the cathodic polarization curves for the electrodeposition of nickel, nickel–thallium and thallium powders from Baths Ni-1, (Ni-Tl)1 and Tl-1, respectively. Inspection of this figure reveals that the electrodeposition of thallium is attended by the highest polarization and the polarization curve of the alloy is closer to that of nickel. This indicates a considerable ennobling of the deposition potential of thallium in the alloy and the feasibility of formation of nickel–thallium solid solutions [10].

The electrodeposition of the alloy from Bath (Ni–Tl)1 has the disadvantage that a dark brown suspension of Tl_2O_3 [11] is formed at the anode and dispersed into the bulk of the bath. The formation of this oxide was observed by other investigators [4, 12] and in this study it could be controlled by the concentration of ammonium sulphate and the pH of the bath. As the concentration of ammonium sulphate decreases in Baths (Ni–Tl)1–4, the formation of Tl_2O_3 decreases considerably and the polarization curves of the alloy deposition shift to less negative values (Fig. 2). This could be caused by the increase of concentration of both Ni^{2+} and Tl^{+} free ions in the bath

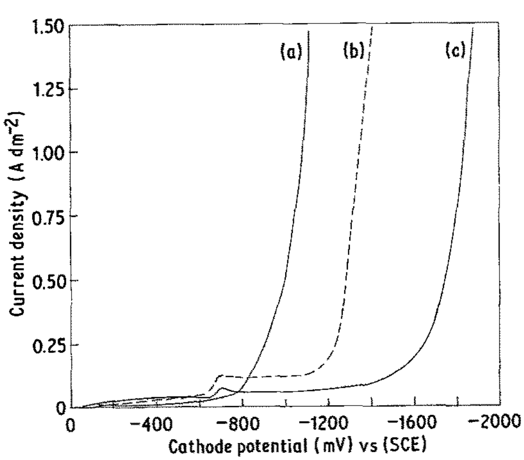

Fig. 1. Polarization curves for nickel, nickel–thallium alloy and thallium electrodeposition from Baths (a) Ni-1, (b) (Ni–Tl) 1 and (c) Tl-1.

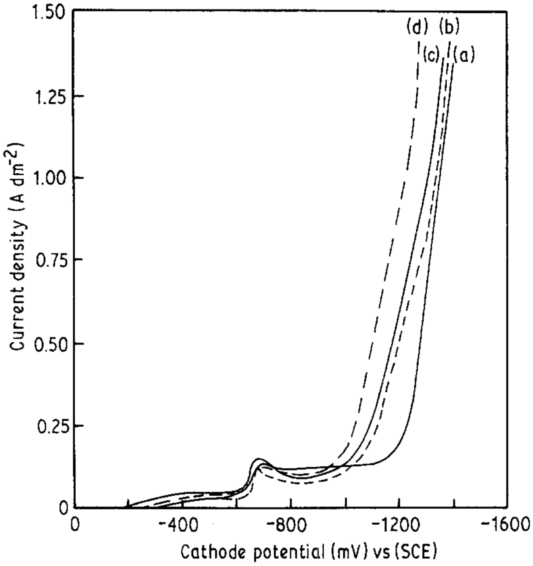

Fig. 2. Polarization curves for nickel–thallium alloy electrodeposition from Baths (a) (Ni–Tl)1, (b) (Ni–Tl)2, (c) (Ni–Tl)3 and (d) (Ni–Tl)4.

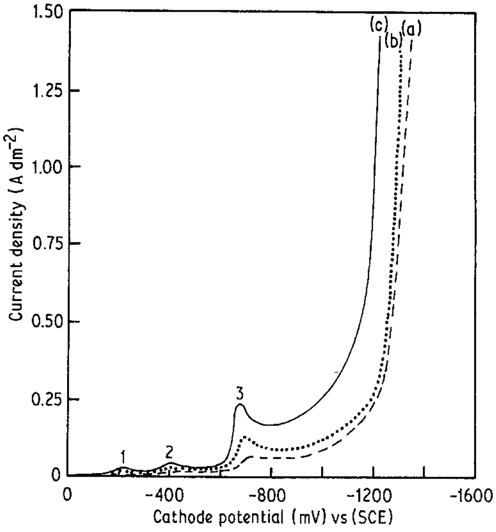

Fig. 3. Polarization curves for nickel–thallium alloy electrodeposition from Baths (a) (Ni–Tl)5, (b) (Ni–Tl)3a and (c) (Ni–Tl)6.

as they form a variety of complexes with the ammonium ions. However, Tl^+–ammonium complexes are more stable and have stability constants $\log K_1 = 4.6$ and $\log \beta_4 = 13$; whereas Ni^{2+}–ammonium complexes are characterized by stability constants of $\log K_1 = 3$ and $\log \beta_4 = 7.98$ [13]. The concentration of ammonium sulphate in Bath (Ni–Tl)3 was found to be suitable for prevention of Tl_2O_3 formation during electrodeposition. Therefore, the composition of Bath (Ni–Tl)3 was chosen to examine the effect of varying the concentration of Tl^+ ion (in the bath) on the characteristics of the electrodeposition process and the alloy deposits.

At concentrations of TiCl higher than 0.01 mol l^{-1}, as in the case of Bath (Ni–Tl)6, the formation of Tl_2O_3 was observed again at the anode and could be prevented by lowering the pH of the bath to 3. Accordingly, to enable a fair comparison, the pH of the three Baths (Ni–Tl)5, 3 and 6 was lowered to 3 by addition of concentrated H_2SO_4 (98%) and Bath (Ni–Tl)3 was denoted as Bath (Ni–Tl)3a. However, the influence of the pH of the bath will be examined in fuller detail in a subsequent article dealing with the effects of the operating variables on the characteristics of nickel–thallium alloys.

Fig. 3 shows that as the concentration of Tl^+ ion increases in Bath (Ni–Tl)5, 3a and 6, respectively, the polarization curves of nickel–thallium alloy deposition shift to less negative values. However, this could be attributed to the decrease of the concentration polarization of the less noble metal [14]. The three peaks denoted by 1, 2 and 3 that appear in the underpotential region (see Fig. 3) could be ascribed to the specific adsorption of Tl^+ ions onto the cathode surface prior to the electrodeposition of the alloy [15]. Moreover, the height of each adsorption peak increases and the potential corresponding to a peak shifts to less negative values with increasing concentration of Tl^+ ion in the bath. The latter observation agrees with the Nernst equation and similar results were obtained during the individual electrodeposition of thallium powders [9]. A correlation between the electrodeposition valency (of thallium) and the difference in electronegativities of substrate and adsorbate indicated a nearly complete discharge of the absorbed Tl^+ ions [16, 17]. Therefore, the three peaks 1, 2 and 3 could be due to the building up of three successive monolayers of Tl-adatoms.

3.2. *Alloy composition*

As can be seen in Fig. 4, the composition of the electrodeposited alloy powders is not affected

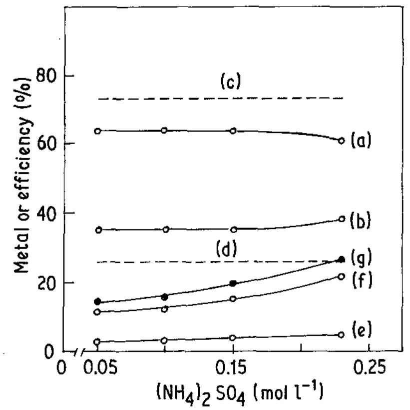

Fig. 4. Effect of ammonium sulphate concentration on the composition curves of (a) thallium and (b) nickel in the alloy; the partial current efficiencies of (e) thallium and (f) nickel in the alloy and the total efficiency (g) of the alloy. The broken lines represent the composition reference lines of (c) thallium and (d) nickel. $i = 6.665$ A dm^{-2} and $t = 10$ min.

considerably by increasing the concentration of ammonium sulphate in Baths (Ni–Tl)4–1. This is a general trend with the single-complex type of alloy deposition bath [18]. However, a slight decrease of the thallium content in the alloy is observed especially at higher concentrations of ammonium sulphate. This could be due to the relatively higher stability of Tl$^+$–ammonium complex ions than those of nickel [13]. The data show also that the composition curve of nickel lies above its composition reference line, that represents the metal-percentage of nickel in the bath, indicating that nickel is the preferentially depositable metal. This result is in good agreement with the result that the polarization curve of the alloy deposition is closer to that of nickel (see Fig. 1).

Electrodeposition of nickel–thallium alloys was carried out from some baths of similar compositions to Bath (Ni–Tl)3a but with various ratios of nickel-to-thallium concentrations. Fig. 5 illustrates the relation between the metal-percentage of nickel or thallium in these baths and the nickel or thallium percentages in the electrodeposited alloy powders. The data reveal that the percentage of either metal in the alloy increases with increasing metal-percentage in the bath. In addition, the slow change in the composition of the alloy with variation of the metal-percentage of nickel in the bath is characteristic of the irregular deposition system [18].

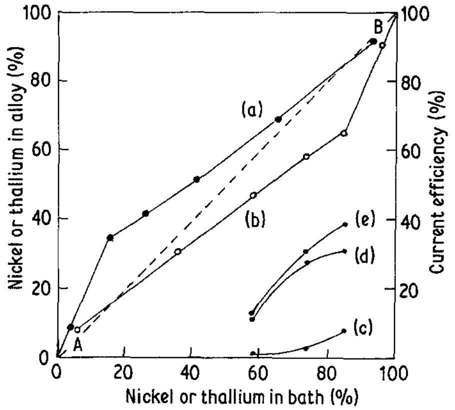

Fig. 5. Effect of the metal-percentage of nickel or thallium in the bath on the percentage of (a) nickel or (b) thallium in the alloy. The broken line AB represents the composition reference of nickel or thallium. The effect of increasing the metal-percentage of thallium in Baths (Ni–Tl)5, 3a and 6 is shown on the partial efficiencies of (c) thallium and (d) nickel and the total efficiency (e) of the alloy. $i = 6.665$ A dm^{-2} and $t = 10$ min.

3.3. *Current efficiency*

As can be seen in Fig. 4, the main effect of an increase of ammonium sulphate in Baths (Ni–Tl)4–1 is to increase the partial efficiency of nickel and hence the deposition efficiency of the alloy without appreciably affecting the efficiency of thallium deposition. These results could be ascribed to the increase of the specific conductance of the baths (Table 1) and agree with the increase of the nickel percentage of the alloy deposits (Fig. 4). In addition, the partial efficiency of thallium is relatively lower than that of nickel. This could be due to the fact that thallium forms a more stable Tl$^+$–ammonium complex than nickel [13] and its deposition is accompanied by a greater polarization (see Fig. 1). Nevertheless, Fig. 4 reveals that the thallium per cent in the alloy is higher than that of nickel. This could be explained by the large difference in the electrochemical equivalents of Ni^{2+} (1.095 g A^{-1} h^{-1}) and Tl$^+$ ions (7.625 g A^{-1} h^{-1}). However, a feature worthy of attention is that the current efficiency of the alloy deposition from Bath (Ni–Tl)1 which equals 27.2% is greater than the efficiencies of either nickel (7.2%) or thallium (6.6%) from the corresponding Baths Ni-1 or Tl-1, respectively.

Fig. 5 shows that on increasing the metal-

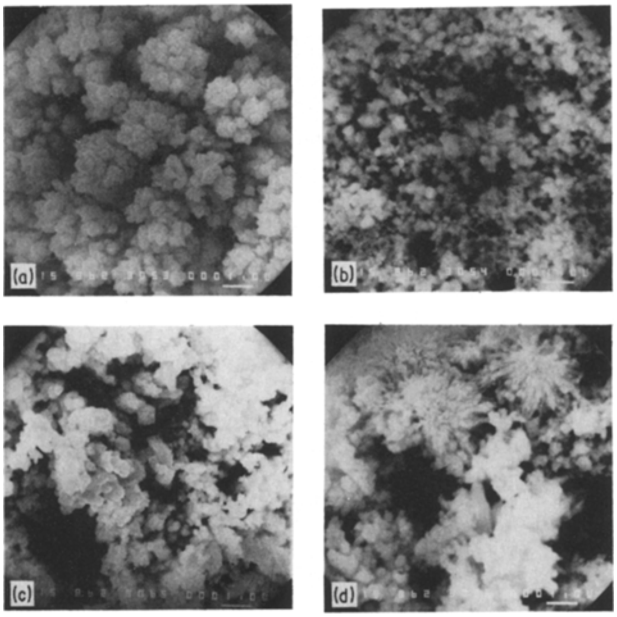

Fig. 6. Electron micrographs of nickel from Bath (a) Ni-1 and nickel–thallium alloys from Baths (b) (Ni–Tl)1, (c) (Ni–Tl)4 and (d) (Ni–Tl)5. $i = 6.665\ \mathrm{A\,dm^{-2}}$, $t = 10$ min and magnification × 6400.

percentage of thallium in Baths (Ni–Tl)5, 3a and 6, respectively, the partial cathodic efficiencies of nickel and thallium increase in the same sense leading to an increase of the efficiency of the alloy deposition. These changes in the current efficiency are in a direction which increases the thallium per cent of the alloy (Fig. 5). These results could be explained by the marked increase of the specific conductance of the baths (Table 1) and shifting of the polarization curves of the alloy deposition to more noble values (Fig. 3).

3.4. *Surface morphology*

Electron micrographs of the as-deposited nickel and some nickel–thallium alloy powders are shown in Fig. 6. The nickel powder from Bath Ni-1 forms in nodular-shaped dendritic clusters (Fig. 6a). The inclusion of thallium in Bath (Ni–Tl)1 results in the formation of a more disperse and finer particle size of the alloy powder (Fig. 6b) than that of the individual nickel. A comparison between Figs. 6b and c shows that the particle size of the dendritic alloy deposits increases with lowering the concentration of ammonium sulphate in Baths (Ni–Tl)1–4, respectively. This could be due to the decrease of the overpotential of the alloy deposition (Fig. 2). Such a condition favours enlargement of the particle size of the deposit rather than enhancement of the nucleation density [19, 20]. A regular trend is shown of decreasing particle size of the alloy powders with decreasing concentration of Tl^+ ion in Baths (Ni–Tl)6, 3a and 5, respectively. This effect is depicted in Fig. 6d which shows the morphology of the alloy powder obtained from Bath (Ni–Tl)5. However, the above-mentioned feature could be correlated to the depletion of Tl^+ ions in the cathode film and the corresponding increase of the concentration polarization (Fig. 3) which promotes the nucleation density and hence produces a deposit of finer particle size [14].

3.5. *X-ray diffractometry*

X-ray diffraction studies were carried out on the alloy powders electrodeposited from some baths having a similar composition to Bath (Ni–Tl)3a but with various ratios of nickel to thallium contents. The relationships between the lattice parameters and the percentage alloy composition are illustrated in Fig. 7. The increase of the lattice parameter of nickel (f c c) with increasing the thallium content of the alloy up to an upper limit of 8% indicates the formation of nickel–thallium solid solution (α-phase). On increasing the thallium content over the range 8–47%, the lattice para-

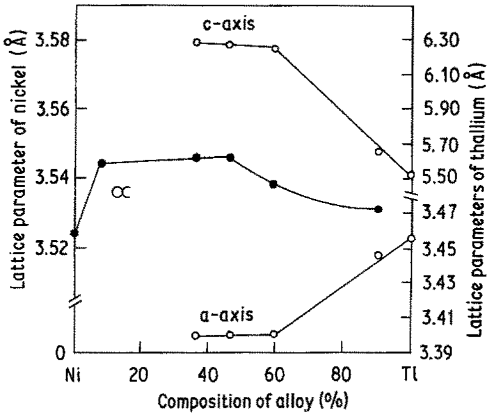

Fig. 7. Variations of the lattice parameters of the f c c α(Ni) and the h c p β(Tl) alloy phases with composition of the alloy. $i = 6.665$ A dm^{-2} and $t = 60$ min.

meter of the α-phase alloy remains constant. The point at which the curve becomes horizontal indicates the limiting composition of the α-phase and the beginning of the formation of an additional phase. Similar behaviour of an electrodeposited silver–thallium alloy was reported by earlier researchers [21]. Then, the lattice parameter decreases gradually with the increase of thallium content of the alloy to about 90%. This could be due to segregation of the α-phase into thallium-depleted nickel alloy and metallic thallium. This suggestion is confirmed by the detection of a variety of Tl_2O and Tl_2O_3 contaminations, as revealed by X-ray analysis, in the electrodeposited alloys over the composition range mentioned above. The occurrence of these oxides is probably due to the ease of oxidation of the segregated thallium by air at room temperature [4].

On the other hand, the lattice parameters of thallium (h c p) vary approximately linearly with increase of the nickel content of the alloy up to a limiting composition of 40% nickel. This change is in accordance, to a great extent, with Vegard's law [18] and confirms the formation of thallium–nickel solid solution (β-phase). The lattice parameters of the β-phase alloy remain constant over the range 40–63% nickel. This indicates the formation of two-phase alloy with the composition of the β-phase remaining constant. The overlapping of the lattice parameter curves shows that a mixture of the α and β-phases occur in the alloys deposited over the range of composition 37–90% of thallium. These results agree with the general features of the phase diagram of the thermally prepared nickel–thallium alloys [22].

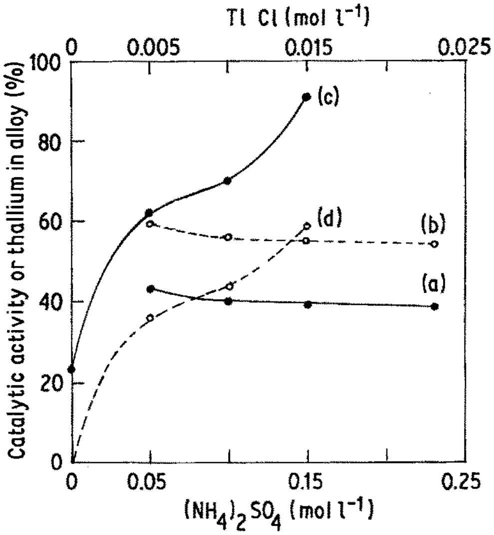

Fig. 8. Effect of the concentration of ammonium sulphate in Baths (Ni–Tl)4–1 on (a) the catalytic activity and (b) the thallium per cent of the alloy powders. Effect of the concentration of thallium chloride in Baths (Ni–Tl)5, 3a and 6 on (c) the catalytic activity and (d) the thallium per cent of the alloy powders. $i = 6.665$ A dm^{-2} and $t =$ 60 min.

3.6. *Catalytic activity*

The percentage decomposition of 0.4% H_2O_2 solution on the as-deposited alloy powders was measured and the results, expressed as D%, are illustrated in Fig. 8. Inspection of this figure shows that as the concentration of ammonium sulphate increases in Baths (Ni–Tl)4–1, D% on the electrodeposited alloy powders decreases slightly. In addition, a comparison between Curves a and b of Fig. 8 depicts a parallelism between the decrease of the catalytic activity and the thallium per cent in the alloy. An obvious feature of Fig. 8 is that as the concentration of Tl^+ ion increases in Baths (Ni–Tl)5, 3a and 6, respectively, there is a marked increase of D% on the electrodeposited alloy powders. Again, a correlation between the increase of the catalytic activity (Curve c) and the thallium per cent in the alloy (Curve d) could be observed. However, it is worth mentioning that D% on any of the examined nickel–thallium alloy powders is higher than D% (23.5%) on the pure nickel powder deposited from Bath Ni-1, under the same conditions. On the other hand, *D*% of the pure thallium powder electrodeposited from Bath Tl-1 is almost 100% but unfortunately about 80% of the metal is oxidized to Tl^+ ions in the presence of 0.4% H_2O_2 solution. In contrast, neither the nickel nor the nickel–thallium alloy powders are oxidized. Therefore, the pure thallium powder could not be considered as a catalyst for the decomposition of H_2O_2.

4. Conclusions

The electrodeposition of nickel–thallium alloy powders from acidic sulphate baths belongs to the irregular deposition system with nickel being the more noble metal. Nickel–thallium solid solutions could be formed and the occurrence of the α(Ni) phase and/or the β(Tl) phase depends on the percentage composition of the alloy.

The inclusion of small amounts of thallium in the alloy leads to dispersion and particle refinement of the deposit in comparison to that of pure nickel. Under identical conditions, the current efficiency and the catalytic activity of the alloy powders are much higher than those of pure nickel powder prepared from a bath of similar composition. A regular trend of increasing catalytic activity with increase of the thallium content of the alloy is observed.

Under the present experimental conditions, the composition of Bath (Ni–Tl)6 seems to be the optimum; it operates with a current efficiency of about 37% and the alloy powders produced are characterized by a catalytic activity of 91.5%.

References

[1] W. G. Parks and I. M. Le Baron, *J. Phys. Chem.* **42** (1938) 125.

[2] E. Raub and F. Sautter, *Metalloberfläche* **13** (1959) 129.

[3] G. R. Pobedimskii and A. I. Zhikharev, *Chem. Abs.* 69 (1968) 102413.

[4] A. Brenner, 'Electrodeposition of Alloys', Vol. II (Academic Press, New York, 1963) p. 168.

[5] V. M. Kochengarov and V. D. Samuilenkova, *Chem. Abs.* 67 (1967) 28689.

[6] S. Wakabayashi, A. Murata and N. Wakabayashi, *Plat. Surf. Finish.* 69 (1982) 63.

[7] G. R. Pobedimskii, *Chem. Abs.* 63 (1965) 5230.

[8] A. M. Abd El-Halim and R. M. Khalil, *Surf. Technol.* in press.

[9] A. M. Abd El-Halim and R. M. Khalil, *Surf. Technol.* in press.

[10] E. Raub and K. Müller, 'Fundamentals of Metal Deposition', (Elsevier, Amsterdam, 1967) p. 136.

[11] F. A. Cotton and G. Wilkinson, 'Advanced Inorganic Chemistry', (Wiley, New York, 1972) p. 263.

[12] I. A. Atanasiu and I. C. Raducanu, *Chem. Abs.* 68 (1968) 110763.

[13] L. G. Sillén and A. E. Martell, 'Stability Constants of Metal Ion Complexes', Chemical Society Special Publication 25 (1971) p. 84.

[14] A. M. Abd El-Halim, *J. Appl. Electrochem.* 14 (1984) 587.

[15] A. M. Abd El-Halim, K. Jüttner and W. J. Lorenz, *J. Electroanal. Chem.* **106** (1980) 193.

[16] J. W. Schultze and F. D. Koppitz, *Electrochim. Acta* **21** (1967) 327.

[17] *Idem, ibid.* **21** (1967) 337.

[18] A. Brenner, 'Electrodeposition of Alloys', Vol. I (Academic Press, New York, 1963) pp. 94, 80–82, 195.

[19] S. Itoh, N. Yamazoe and T. Seiyama, *Surf. Technol.* **5** (1977) 27.

[20] A. M. Abd El-Halim and M. I. Sobahi, *ibid.* **19** (1983) 45.

[21] E. Raub and F. Sautter, *Metalloberfläche* **10** (1955) 145.

[22] M. Hansen, 'Constitution of Binary Alloys', (McGraw-Hill, New York, 1958) p. 1053.